Human stem cell–derived neurons and astrocytes to detect novel auto-reactive IgG response in immune-mediated neurological diseases

Amandine Mathias[1], Sylvain Perriot[1], Samuel Jones[1],
Mathieu Canales[1], Raphaël Bernard-Valnet[2], Marie Gimenez[1],
Nathan Torcida[1], Larise Oberholster[1], Andreas F. Hottinger[3],
Anastasia Zekeridou[4], Marie Theaudin[2], Caroline Pot[1,2]
and Renaud Du Pasquier[1,2]*

[1]Laboratories of Neuroimmunology, Neuroscience Research Center and Division of Neurology,
Department of Clinical Neurosciences, Lausanne University Hospital and Lausanne University,
Epalinges, Switzerland, [2]Service of Neurology, Department of Clinical Neurosciences, Lausanne
University Hospital and University of Lausanne, Lausanne, Switzerland, [3]Lundin Family Brain Tumor
Research Centre, Department of Clinical Neurosciences and Oncology, Lausanne University Hospital
and University of Lausanne, Lausanne, Switzerland, [4]Department of Laboratory Medicine and
Pathology and Department of Neurology, Center for MS and Autoimmune Neurology, Mayo Clinic,
Rochester, MN, United States

Background and objectives: Up to 46% of patients with presumed autoimmune limbic encephalitis are seronegative for all currently known central nervous system (CNS) antigens. We developed a cell-based assay (CBA) to screen for novel neural antibodies in serum and cerebrospinal fluid (CSF) using neurons and astrocytes derived from human-induced pluripotent stem cells (hiPSCs).

Methods: Human iPSC-derived astrocytes or neurons were incubated with serum/CSF from 99 patients [42 with inflammatory neurological diseases (IND) and 57 with non-IND (NIND)]. The IND group included 11 patients with previously established neural antibodies, six with seronegative neuromyelitis optica spectrum disorder (NMOSD), 12 with suspected autoimmune encephalitis/paraneoplastic syndrome (AIE/PNS), and 13 with other IND (OIND). IgG binding to fixed CNS cells was detected using fluorescently-labeled antibodies and analyzed through automated fluorescence measures. IgG neuronal/astrocyte reactivity was further analyzed by flow cytometry. Peripheral blood mononuclear cells (PBMCs) were used as CNS-irrelevant control target cells. Reactivity profile was defined as positive using a Robust regression and Outlier removal test with a false discovery rate at 10% following each individual readout.

Results: Using our CBA, we detected antibodies recognizing hiPSC-derived neural cells in 19/99 subjects. Antibodies bound specifically to astrocytes in nine cases, to neurons in eight cases, and to both cell types in two cases, as confirmed by microscopy single-cell analyses. Highlighting the significance of our comprehensive 96-well CBA assay, neural-specific antibody binding was more frequent in IND (15 of 42) than in NIND patients (4 of 57) (Fisher's exact test, $p = 0.0005$). Two of four AQP4+ NMO and four of seven definite AIE/PNS with

intracellular-reactive antibodies [1 GFAP astrocytopathy, 2 Hu+, 1 Ri+ AIE/PNS)], as identified in diagnostic laboratories, were also positive with our CBA. Most interestingly, we showed antibody-reactivity in two of six seronegative NMOSD, six of 12 probable AIE/PNS, and one of 13 OIND. Flow cytometry using hiPSC-derived CNS cells or PBMC-detected antibody binding in 13 versus zero patients, respectively, establishing the specificity of the detected antibodies for neural tissue.

Conclusion: Our unique hiPSC-based CBA allows for the testing of novel neuron-/astrocyte-reactive antibodies in patients with suspected immune-mediated neurological syndromes, and negative testing in established routine laboratories, opening new perspectives in establishing a diagnosis of such complex diseases.

1 Introduction

The discovery of central nervous system (CNS)–reactive auto-antibodies (Abs) has significantly transformed clinical practice and therapeutic approaches in clinical neurosciences, particularly in the management of neurological disorders such as paraneoplastic syndromes (PNS), autoimmune encephalitis (AIE), or neuromyelitis optica spectrum disorders (NMOSD). Auto-Abs can be identified in diseases with various etiologies including malignancies, auto-immune conditions, and post-infectious syndromes (1, 2). In the context of suggestive clinical and neuro-radiological features, their precise identification has a profound impact on guiding therapeutic strategies ranging from immunotherapies to cancer therapies (3, 4). Nevertheless, 7%–46% of the patients with definite or probable autoimmune limbic encephalitis (LE), as defined by 2016 criteria (3), still remain seronegative for all currently known neural antigens (Ag) (3, 5–8). This suggests that new auto-Abs targets are yet to be discovered.

Similarly, 6%–16% of NMOSD patients diagnosed according to the 2015 criteria are seronegative for AQP4 Abs and MOG Abs (9, 10). In comparison to seropositive cases, in seronegative AIE or NMOSD, the diagnosis is often delayed, hindering appropriate therapeutic measures and impacting outcomes. Thus, there is a need for an improved and expedited Ag discovery platform (7, 11–13).

The detection of novel CNS-reactive Abs crucially depends on the Ag source. Preserving the native configuration of the CNS Ag is paramount. Conventional approaches include protein, tissue, or cell-based assays (CBAs). Protein-based assays, such as Western blot, often alter protein configuration, significantly reducing the likelihood of detecting novel antigenic targets for auto-Abs that depend on conformational structures to bind (e.g., muscle acetylcholine receptor Abs) (14, 15). Immunofluorescence/immunohistochemistry on animal brain tissues (e.g., rat/mouse/non-human primate) offers the advantage of preserving some native configuration. However, the use of animal-derived Ags in this assay may prevent the detection of human-specific Abs. However, human material is scarce (brain biopsies are rarely performed) and available specimens are often in degraded conditions (e.g., autopsy) (16–18). Last, CBA using human CNS primary cells would probably be efficient in binding CNS-specific auto-Abs as the native conformation of human proteins is preserved. Nevertheless, here again, the difficulty to obtain human CNS primary cells represents a real burden in the quest for CNS-specific Abs (19).

Human induced pluripotent stem cell (hiPSC)-derived CNS cells emerge as a solution to overcome the limited access to human CNS tissue or CNS primary cells (20). In this study, we describe a unique CBA combining human iPSC-derived neurons and astrocytes as a virtually unlimited source of naturally expressing neural Ags to screen for the presence of novel CNS-specific Abs in the serum and cerebrospinal fluid (CSF) from patients with suspected immune-mediated neurological conditions.

2 Materials and methods

2.1 Study subjects

Patients were enrolled from 2004 to 2022 as part of the ongoing open study COOLIN BRAIN (Cohort Observational Longitudinal Inflammatory Biological Radiological Investigations) aiming at characterizing neuro-immune disorders. Data collection includes clinical, biological, and radiological characteristics. Patients were

categorized as follows: 1. AQP4+ and seronegative NMOSD following the 2015 IPND criteria (12); 2. patients diagnosed with definite or suspected AIE/PNS fulfilling diagnostic criteria defined by Graus et al. (3, 21) (autoimmune encephalitis associated or not with a paraneoplastic syndrome; AIE/PNS); 3. other inflammatory neurological disorders (OIND); and 4. non-inflammatory neurological disorders (NIND) as controls (see "results section" for further details). The results of neural-/glial-specific auto-Ab testing performed for NMOSD and AIE/PNS patients were collected from reference centers (Labor Krone, Bad Salzuflen, Germany; Clinical Immunology and allergy, Sion, Switzerland; Zurich University Hospital; Switzerland; Geneva University Hospital, Switzerland; Bern University Hospital, Switzerland; Hospital Clínic of Barcelona, Barcelona, Spain; Hospices Civils de Lyon, Lyon, France). All information were collected from analyses performed at the time of diagnosis and gathered from patient medical files. Patients tested positive for non-CNS–specific auto-Abs in validated diagnostic laboratories at the time of sample collection, such as antinuclear factor (ANA), rheumatoid factor, anti-neutrophilic cytoplasmic Abs (ANCA), anti-double strand DNA Abs (dsDNA), or antiphospholipid Abs were excluded to avoid discussion on whether the neural-reactive Abs we detect with our hiPSC–derived neural CBA might also recognize non-CNS–restricted Ags. All samples (serum or CSF) were collected, processed, and stored by the lab through standardized procedures attesting high sample quality (Swiss biobanking platform, Vita label: BBH-NI). This study received approval by our institution's review board (protocol 2018–01622, COOLIN'BRAIN cohort), and all subjects gave written informed consent before study initiation.

2.2 Human iPSC-derived CNS cells: donors, differentiation, and culture

Peripheral blood mononuclear cells (PBMCs) of two healthy donors were converted into fully characterized hiPSC and neural precursor cells (NPCs) as described previously (age/sex: HD#002: 50/M, cell line ID: LNISi002-B; HD#003: 49/F, cell line ID: LNISi003-A) (22–24). All donors gave their written informed consent according to regulations established by the responsible ethics committee (CER-VD 2018–01622). Astrocytes were obtained by differentiating NPC in serum-free medium following standardized procedure (22, 23). Media were changed every 2–3 days, and cells were passed when at confluence. Neurons were obtained by lentiviral transduction of lentiviruses encoding for human Neurogenin 2 into hiPSC-derived NPC and induction of expression (25). Briefly, NPC were plated on poly-L-ornithine/laminin-coated flasks at 50,000 cells/cm^2 in 2 μg/ml laminin-supplemented neural expansion medium (DMEM/F-12 + Glutamax, Gibco®; 1× N-2 supplement, Gibco®; 1× B27 supplement without vitamin A, Gibco®; 10 ng/ml FGF-2, PeproTech; 10 ng/ml EGF, Miltenyi). NPC were then transduced with a VSV-G-pseudotyped lentivirus [carrying pCW57.1 plasmid from Addgene # 41393 (gift from David Root) modified to include hNGN2 under the doxycycline promoter]. To select for transduced NPC (NGN2-NPC), neural expansion medium was supplemented

with 2 μg/mL puromycin after 24h and changed every 2–3 days. NGN2-NPC was amplified and frozen until use. Neuronal differentiation was induced by culturing NGN2-NPC in neural differentiation medium (DMEM/F-12 + Glutamax, Gibco®; 1× N-2 supplement, Gibco®; 1× B27 supplement without vitamin A, Gibco®) supplemented with doxycycline (2 μg/ml). Medium was changed every other day for 6–8 days. All cells were cultivated at 37°C in 5% CO_2. Importantly, astrocyte and neuron differentiation profiles were assessed by routine RT-qPCR (22, 26, 27) and immunofluorescence (22, 26, 28, 29), confirming the expression of astrocytic or neuronal markers, respectively (see Supplementary Table S1 for primer list, Supplementary Table S2 for the list of reagents used for immunofluorescence stainings, Supplementary Figure S1 for representative results from differentiation profile assessments).

2.3 96-well hiPSC-derived CNS cell-based assay (96-well hiPSC-derived CNS CBA)

Human iPSC-derived astrocytes and NGN2-NPC were plated on poly-L-ornithine/laminin pre-coated 96-well plates (flat bottom Costar® tissue-treated plates) at 30,000 cells/cm^2 the day preceding the CBA for astrocytes and at 20,000 cells/well 6–8 days before the CBA for NGN2-NPC to allow in-situ neuronal differentiation, respectively.

To detect both extra- and intracellular-bound Abs, cells were directly fixed with 4% PFA in PBS for 60 min at room temperature (RT) for astrocytes or 100% cold ethanol for neurons for 10 min. After washing all wells with PBS, cells were then permeabilized and non-specific sites were blocked using Perm./Block-Buffer (5% NGS + 0.2% saponin + 0.1% triton X100 in PBS) for 20 min at RT. Wells were then washed with PBS and positive controls [anti-CD44 Abs (Miltenyi) for astrocytes; anti-β-tubulin III (Biotechne) Abs for neurons], negative controls (Perm./Block-Buffer only, without serum/CSF nor primary commercial Abs) and patient samples were added into the wells for 35 min at RT. Positive controls and serum and CSF samples were diluted in Perm./Block-buffer for extra- and intracellular staining. All serum and CSF samples were run as duplicates and were normalized for their individual IgG concentration (final concentrations tested to minimize unspecific background signal: 15 μg/ml for serum and 1.5 μg/ml for CSF). Briefly, after normalization of total IgG concentrations, the astrocyte and neuron reactivities were assessed in a preliminary cohort of AQP4+ NMO and definite anti-Hu+ AIE/PNS with known astrocyte and neuronal reactivity (diagnostic laboratories) versus NIND subjects (serum/CSF) and healthy donors (HDs) (serum only). These preliminary experiments allowed to define the total IgG concentration associated with the best signal-to-noise ratio (data not shown). As the median IgG indexes for astrocytes and neurons in the HD group (serum only) were comparable to those in the NIND group and considering that no lumbar punctures were performed in HD (ethical reasons), we kept only the NIND group as the control group for further IgG binding profile evaluation in both compartments (CSF and serum). Total IgG quantification was determined by the Laboratory of Immunology and Allergy (LIA) of Lausanne, (CHUV, Switzerland). Median IgG

concentrations were 10.6 mg/mL in the serum and 32.2 µg/mL in the CSF corresponding to a final median dilution of 1/700 [range: 1/133–2540] and 1/22 [range: 1/2; 1/300], for serum and CSF evaluation in our 96-well CBA, respectively.

Biotinylated human anti-IgG secondary Abs also diluted in Perm./Block-buffer were then incubated for 30 min at RT in order to detect the presence of bound Abs. After extensive washes in PBS, fluorescent phycoerythrin (PE)–labeled streptavidin was added for another 30 min at RT. Negative controls correspond to anti-human IgG detection Abs with PE-labeled streptavidin only. Finally, cells were counterstained with 4′, 6-diamidino-2-phenylindole (DAPI) diluted in PBS for 10 min at RT. Both controls and samples were run in duplicates. Overall IgG-binding profile was automatically assessed by measuring PE fluorescence intensity (see section Automated IgG binding profile detection of 96-well hiPSC-derived CNS CBA plates). IgG cellular distribution was further characterized by fluorescence microscopy observation (see section IgG binding profile characterization by fluorescence microscopy observation of 96-well hiPSC-derived CNS CBA plates).

2.4 Automated IgG binding profile detection of 96-well hiPSC-derived CNS CBA plates

Detection of fluorescently labeled cells (fluorescence intensity, FI) was automated using a Synergy® H1 (BioTek®) hybrid multimode plate reader and results were analyzed with Gen5 software (BioTek®, v.3.03.14). To take into account the variable number of cells at the bottom of each well, raw FI were normalized, using GraphPad Prism® 9 software [Version 9.5.1(733)] in accordance with the following formula: $IgG index = [Raw\ FI_{PE}(well) — Mean\ FI_{PE}(negative\ controls)]/ FI_{DAPI}(well)$. All wells with restricted number of cells (DAPI signal<2,500) or excessive number of cells (DAPI signal >20,000) were excluded due to possible bias in IgG index calculation. If the coefficient of variation of the duplicates (CV = standard deviation of duplicate/mean of duplicate*100) was above 50%, the duplicate was considered as discrepant and excluded to ensure robustness of subsequent analyses. A z-score of each validated IgG index was then calculated for comparison purposes.

2.5 IgG binding profile characterization by fluorescence microscopy observation of 96-well hiPSC-derived CNS CBA plates

Fluorescence microscopy observations of the 96-well hiPSC-derived CNS CBA was automatized using a high-performance EVOS M7000. Four images were acquired per well. Post-image processing was performed using ZEN 2.3 (Zeiss®, v1.3), ImageJ (NIH, v.1.50b), and CellProfiler (version 4.2.1) Softwares. Image acquisitions were accomplished using identical parameters for specific Abs, negative controls, and patient serum and CSF samples. Images were post-processed identically between all serum samples vs all CSF samples, background levels being specifically adjusted for serum vs CSF. Single-cell IgG-associated fluorescence was measured in each individual picture using CellProfiler (version 4.2.1) (30) and CellProfiler analyst (version 3.0.4) (31) software. Mean single cell FI and z-score per well were then calculated and correlated with automated plate reader readouts (IgG index [z-score]) (Supplementary Figure S2).

2.6 Flow cytometry analyses

Human iPSC-derived astrocytes and neurons were detached and stained as described previously (22, 28, 32). Briefly, detached CNS cells were first stained with Aqua Live/Dead (Life Technologies) for 20 min at 4°C. After fixation and permeabilization in Cytofix/Cytoperm buffer (BD Biosciences), cells were washed with PermWash buffer 1× (BD Biosciences) and stained for 35 min at 4°C with serum or CSF. All serum and CSF samples were normalized for their IgG concentration (final concentration tested 15 µg/ml for serum and 1.5 µg/ml for CSF). Cells were then washed and stained with biotinylated human anti-IgG secondary Abs for 30 min at 4°C followed by PE-labeled streptavidin (same concentrations as for 96-well hiPSC-derived CNS CBA). Negative controls correspond to anti-human IgG detection Abs with PE-labeled streptavidin only.

To ensure that IgG reactivity was restricted to CNS cells, CD3+ T lymphocytes were used as an irrelevant source of primary cells. Briefly, a buffy coat of a healthy donor was obtained from the Lausanne interregional transfusion center and total PBMCs were isolated as described previously (33). PBMCs were then exposed to serum and CSF samples and stained exactly as done for CNS cells except for the addition of an anti-CD3 APC-H7 Ab (BD Biosciences) during the Aqua Live/Dead staining step.

Data were acquired on a LSRII flow cytometer (BD Biosciences) and analyzed with FlowJo software (see Supplementary Figure S3 for gating strategies, version 9.1.11, Treestar) (see Supplementary Figure S3 for gating strategies). IgG median fluorescence intensity (MFI) was used to quantify IgG binding and z-score per sample were then calculated for comparison purposes.

2.7 Tissue indirect immunofluorescence

If a sufficient sample volume was available, serum and/or CSF samples with IgG staining in neurons or astrocytes using our hiPSC-derived CNS cell CBA (seronegative NMOSD, suspected AIE/PNS, OIND, and NIND) were evaluated by indirect immunofluorescence on a mouse tissue composite (TIF) including brain, kidney and enteric neurons and gut [Mayo Clinic Neuroimmunology Laboratory, as previously described (34)].

2.8 Statistical analyses and graphical representations

Both data analysis and creation of figures were performed on R software version 4.3.1 (2023–06-16 ucrt) including specific packages (ggplot2_3.4.3, ggpubr_0.6.0, rstatix_0.7.2, corrplot_0.92). Serum

and CSF outliers with a high probability of an association with CNS-reactive Abs were identified using a robust regression and outlier removal test (ROUT test) with a false discovery rate (FDR) at 10% on calculated IgG index (z-score) or IgG MFI (z-score). Comparisons of outlier frequencies from one to another group were tested using a two-sided Fisher's exact test (p-value: p_F in the text). Correlations between two readouts (96-well plate reader versus microscopy or 96-well plate reader versus flow cytometry) were evaluated using a Spearman's rank correlation test (p-value: p_S in the text). For all statistical analyses, a p-value inferior to 0.05 was considered significant.

3 Results

3.1 Study cohort

One hundred and thirty patients were initially enrolled from 2004 to 2022 (Figure 1). Inclusion criteria encompassed patients with an established diagnosis of definite auto-Ab–related neurological condition; patients with a high probability of suffering from an Ab-related neurological condition but negative for all CNS auto-Abs tested in validated diagnostic laboratories, OIND patients, and NIND patients. Thirty-one patients were positive to non-CNS–specific auto-Abs and were thus excluded from further analyses. Therefore, 99 patients were finally studied. This cohort included 57 NIND control patients and 42 patients with inflammatory neurological diseases (IND). The latter category

included four definite AQP4+ NMO, six seronegative NMOSD, seven definite autoimmune neurological disorders (autoimmune encephalitis associated or not with a paraneoplastic syndrome; AIE/PNS), 12 suspected AIE/PNS, and 13 OIND (Figure 1, Table 1, and Supplementary Tables S3–S7). As part of the validation cohort for the 96-well hiPSC-derived astrocyte CBA, we included five patients with known astrocyte-reactive Abs. This cohort comprised four patients diagnosed with AQP4+ NMO and one patient with GFAP+ astrocytopathy (Figure 1, left end side). For the 96-well hiPSC-derived neuron CBA, the validation cohort included six patients with previously reported neuronal-reactive Abs. These patients had definite autoimmune encephalitis (AIE) or paraneoplastic neurological syndrome (PNS) and were positive for the following neuronal Abs: Hu (n = 2), Ri (n = 1), AK5 (n = 1), NMDAR (n = 1), and anti-PCA-Tr (n = 1) (Figure 1, middle part). A comprehensive analysis was done on the exploratory cohort comprising all seronegative NMOSD, suspected AIE/PNS, OIND, and suffering patients (Figure 1, right end side). Each exploratory patient was tested for the presence of both astrocyte- and neuron-reactive auto-Abs, without any a priori about cellular specificity.

To screen for the presence of CNS-specific Abs in selected patients, hiPSC-derived astrocytes (Figure 2) and neurons (Figure 3) were seeded in 96-well plates and exposed to serum and CSF from the 99 study participants. For a rapid evaluation of the IgG binding profile, measures of the IgG-associated fluorescence intensity were automated at the well level using a fluorescence plate reader. This readout allowed us to identify positive serum or CSF samples (Figures 2A, B, 3A, B). Microscopy observation further

FIGURE 1
Flowchart of the study design followed for patient recruitment. AIE, autoimmune encephalitis; PNS, paraneoplastic syndrome; NMOSD, neuromyelitis optica spectrum disorder. *Non-organ−specific antibodies for example ANA, ANCA, dsDNA, Jo, SSA, SSB. **Neural-/glial−specific auto-antibody testing routinely included in evaluation panels for suspected autoimmune and paraneoplastic disorders. ***Including six AIE/PNS patients with neuronal-reactive antibodies [Hu+ (n = 2), Ri+ (n = 1), AK5+ (n = 1), NMDAR+ (n = 1), anti-PCA-Tr+ (n = 1)].
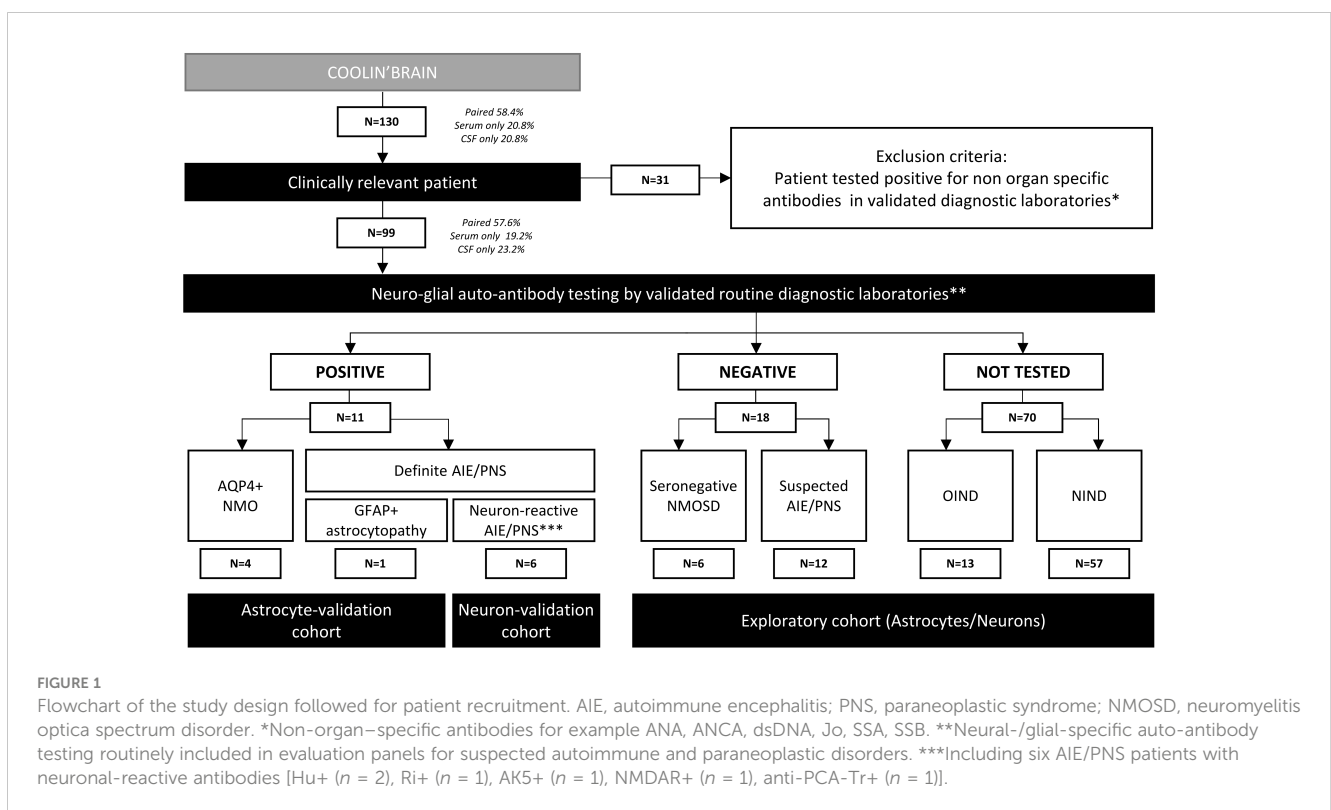
TABLE 1   Clinical data of the 99 patients enrolled in this study.

Group	Diagnosis	Number	M/F ratio	Median age [IQR] (years)	Median disease duration [IQR] (years)
IND	AQP4+ NMO[a]	4	0/4	36.3 [18.3]	7.04 [18.58]
	Seronegative NMOSD[b]	6	1/5	34.9 [9.8]	1.09 [6.23]
	Definite AIE/PNS[c]	7	2/5	59.7 [18.7]	0.11 [0.39]
	Suspected AIE/PNS[d]	12	7/5	66.3 [32.9]	0.18 [0.267]
	OIND[e]	13	5/8	40.4 [24.5]	0.03 [0.54]
NIND[e]		57	17/40	45.3 [24.8]	0.79 [2.63]
Total		**99**	**32/67**	**44.7 [28.9]**	**0.31 [1.98]**

[a]AQP4+ NMO: see Supplementary Table S3 for subject details.
[b]Seronegative NMOSD: see Supplementary Table S4 for subject details.
[c]Definite PNS/AIE: see Supplementary Table S5 for subject details.
[d]Suspected AIE/PNS: see Supplementary Table S6 for subject details.
[e]OIND and NIND: see Supplementary Table S7 for subject details.
IND, inflammatory neurological diseases; PNS, paraneoplastic syndrome; AIE, autoimmune encephalitis; NMOSD, neuromyelitis optica spectrum disorder; MS, multiple sclerosis; OIND, other inflammatory neurological diseases; NIND, non-inflammatory neurological diseases.

confirmed the IgG binding to CNS cells. Indeed, we found that there was a strong significant positive correlation between rapid IgG indexes (z-score, plate reader, and well level) and median IgG intensity microscopy measurements (z-score, microscope, and single cell) (Supplementary Figure S2).

3.2 Astrocytes reactive-antibodies

Relying on the rapid automated plate reader IgG measurements, we identified astrocyte-specific IgG in nine of 36 (25%) IND [patients considered: four AQP4+ NMO and one GFAP+ astrocytopathy for the validation cohort; six seronegative NMOSD, 12 suspected AIE/PNS and 13 OIND as part of the exploratory cohort] versus two of 57 (3.5%) NIND patients (p_F= 0.003; Figure 2A). Astrocyte-reactive Abs were more frequently found in the CSF only (five of 11; 45.4%) than in the serum only (three of 11; 27.3%) or in both serum and CSF together (three of 11; 27.3%). Validating the ability of our 96-well hiPSC-derived astrocyte-based CBA to detect astrocyte-specific IgG, we observed a strong astrocyte signal in the CSF of a patient with autoimmune GFAP astrocytopathy and in the serum and CSF of two patients with NMOSD and AQP4-Abs in a routine reference laboratory at the time of sample collection. Our astrocyte-based CBA was negative in two patients previously diagnosed with AQP4+ NMOSD but tested negative (AQP4+ NMO #4) or with a low AQP4+ Ab titer (AQP4+ NMO #3; 1:32), a titer far higher than the one established in our assay (final serum concentration 15 μg/mL corresponding to a 1:860 dilution for this patient). Most interestingly, using this unique 96-well hiPSC-derived astrocyte CBA, we were able to detect astrocyte-specific IgG in two of six seronegative NMOSD (33.3%), three of 12 suspected AIE/PNS (25%), and one of 13 OIND (7.7%) (Figure 2B and Supplementary Tables S3–S7 for clinical description). These results were further illustrated and confirmed by fluorescence microscopy observations (Figures 2C, D).

3.3 Neuron-reactive antibodies

Similar experiments were conducted using hiPSC-derived neurons. We identified neuron-specific IgG in two of 57 NIND (3.5%) and in eight of 37 (21.6%) IND study patients (p_F= 0.013, Figure 3A) [patients considered: six definite AIE/PNS with neuron-reactive Abs for the validation cohort, six seronegative NMOSD, 12 suspected AIE/PNS, and 13 OIND as part of the exploratory cohort]. Contrasting with astrocyte-reactive IgG, which was detected mostly in the CSF, neuron-specific IgG was found similarly distributed between the two compartments: CSF only in three of 10 (30%) and serum only in four of 10 (40%). Antibodies were detected in both serum and CSF in three of 10 (30%). Such as was done for astrocytes, we enrolled six patients with definite neuron-specific Ab-associated neurological disorders: anti-AK5+ AIE/PNS (n = 1), anti-PCA-Tr+ AIE/PNS (n = 1), anti-NMDAR+ AIE/PNS (n = 1), anti-Hu+ AIE/PNS (n = 2), and anti-Ri+ AIE/PNS (n = 1). We were able to identify three of six AIE/PNS patients (50%), namely, the two Hu+ and the Ri+ AIE/PNS patients.

As part of the exploratory cohort, we selected 12 patients with suspected AIE/PNS who tested negative in validated diagnostic laboratories using all known neural-/glial-specific auto-Ab panels, all patients fulfilling the AIE/PNS criteria (3, 21). Of those 12 patients, nine had an underlying oncological condition (Table 1, Supplementary Table S6 for clinical details). Using this 96-well hiPSC-derived neuron CBA, we were able to detect neuron-specific Abs in four of 12 patients suspected AIE/PNS patients (33.3%). Interestingly, we could also detect neuron-specific Abs in 1/6 seronegative NMOSD (16.7%) (Figure 3B, Supplementary Table S4 for clinical description). These results were further illustrated and confirmed by fluorescence microscopy observations (Figures 3C, D).

Finally, IgG staining patterns of serum/CSF samples from suspected AIE/PNS, seronegative NMOSD, OIND, and NIND patients found to be positive in our hiPSC-derived CNS CBA were evaluated by indirect immunofluorescence on a mouse tissue composite (TIF) if enough serum/CSF remained. None of these
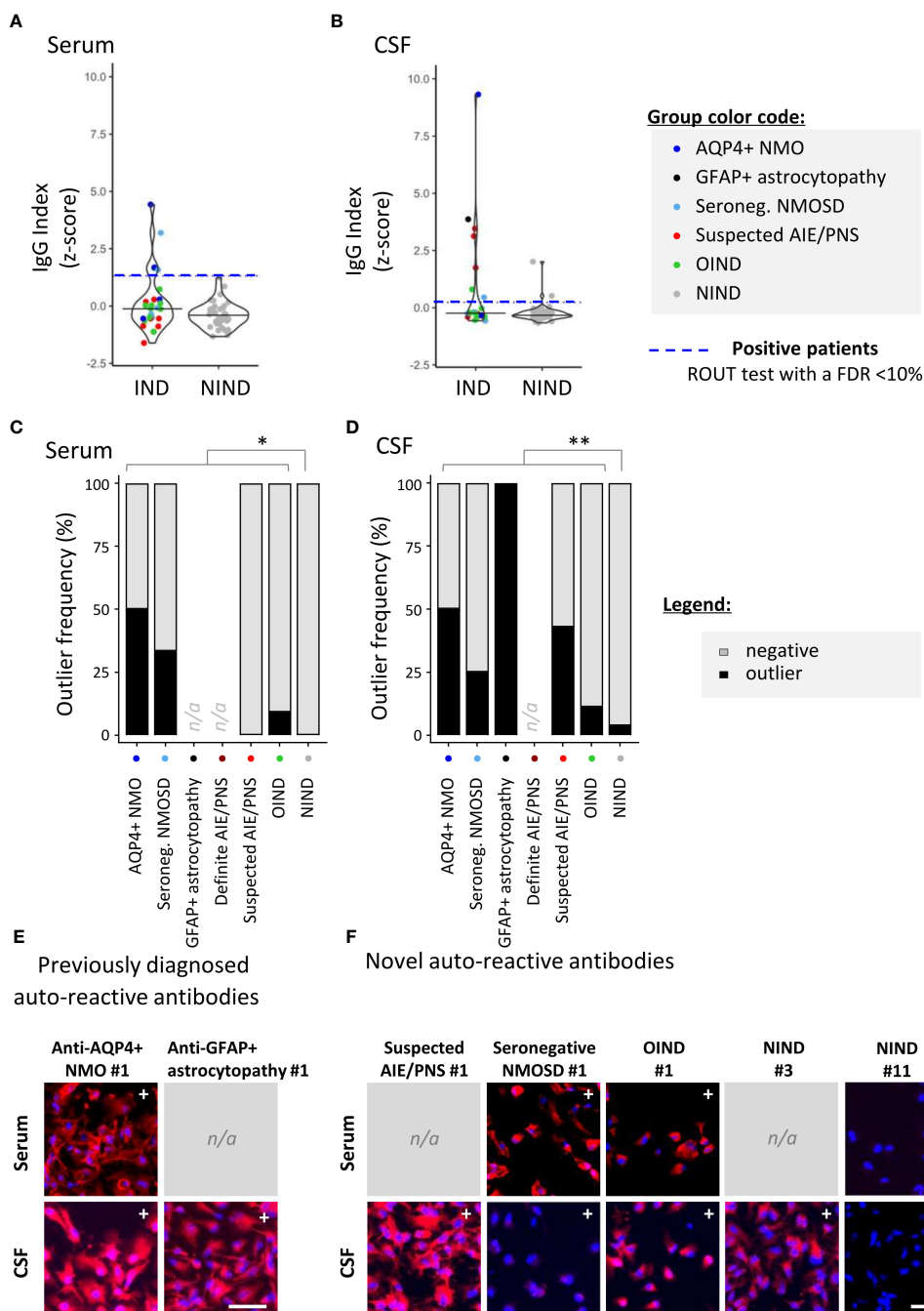
FIGURE 2

Detection of astrocyte-reactive IgG in sera and CSF of patients with a 96-well hiPSC-derived astrocyte cell-based assay (CBA). Human iPSC-derived astrocytes were used to screen for CNS-reactive Abs associated with inflammatory and non-inflammatory neurological syndromes (IND and NIND, respectively). Cells were exposed to selected serum and cerebrospinal fluid (CSF) (Figure 1). IgG-bound to astrocytes were detected in an intracellular 96-well CBA. **(A)** FI were assessed using a Synergy® microplate reader (left, serum; right, CSF). IgG indexes (z-score) are represented (see Methods for details). Each dot represents the mean of duplicates. The black plain lines represent the median of the group. Each clinical subgroups are represented in different colors. The blue dotted line represents the statistically determined limit above which outliers (defined as positive samples) were identified using a ROUT test with an FDR at<10% (see legend for color/group correspondence). Noteworthy, the patient suffering from GFAP+ astrocytopathy (CSF only) is represented in black as the only definite AIE/PNS patient with reported astrocyte-reactivity. **(B)** The frequency of outliers in each clinical subgroups are represented in black as bar graphs in the serum (left panel) or in the CSF (right panel). Differences in outlier frequencies between IND and NIND groups were tested using Fisher's exact test: *, $p< 0.05$; **, $p< 0.01$. **(C, D)** Wells of the astrocyte-based CBA were observed by fluorescence microscopy. Representative microscopic observations are depicted for an AQP4+ NMO patient (expected surface and intracellular IgG pattern) and a patient suffering from GFAP+ astrocytopathy (expected intracellular IgG pattern) tested positive by validated diagnostic laboratories **(C)** and for patients tested negative or not tested by validated diagnostic laboratories [**(D)**, intracellular patterns]. The presence of IgG bound to astrocytes are detected in red, and nuclei staining (DAPI) appears in blue. Symbols (+ or −) depicted in the upper right corner represent the results of CBA either positive outlier (+) or non-outliers (−) sample. White bars represent 50μm. n/a; data not available.
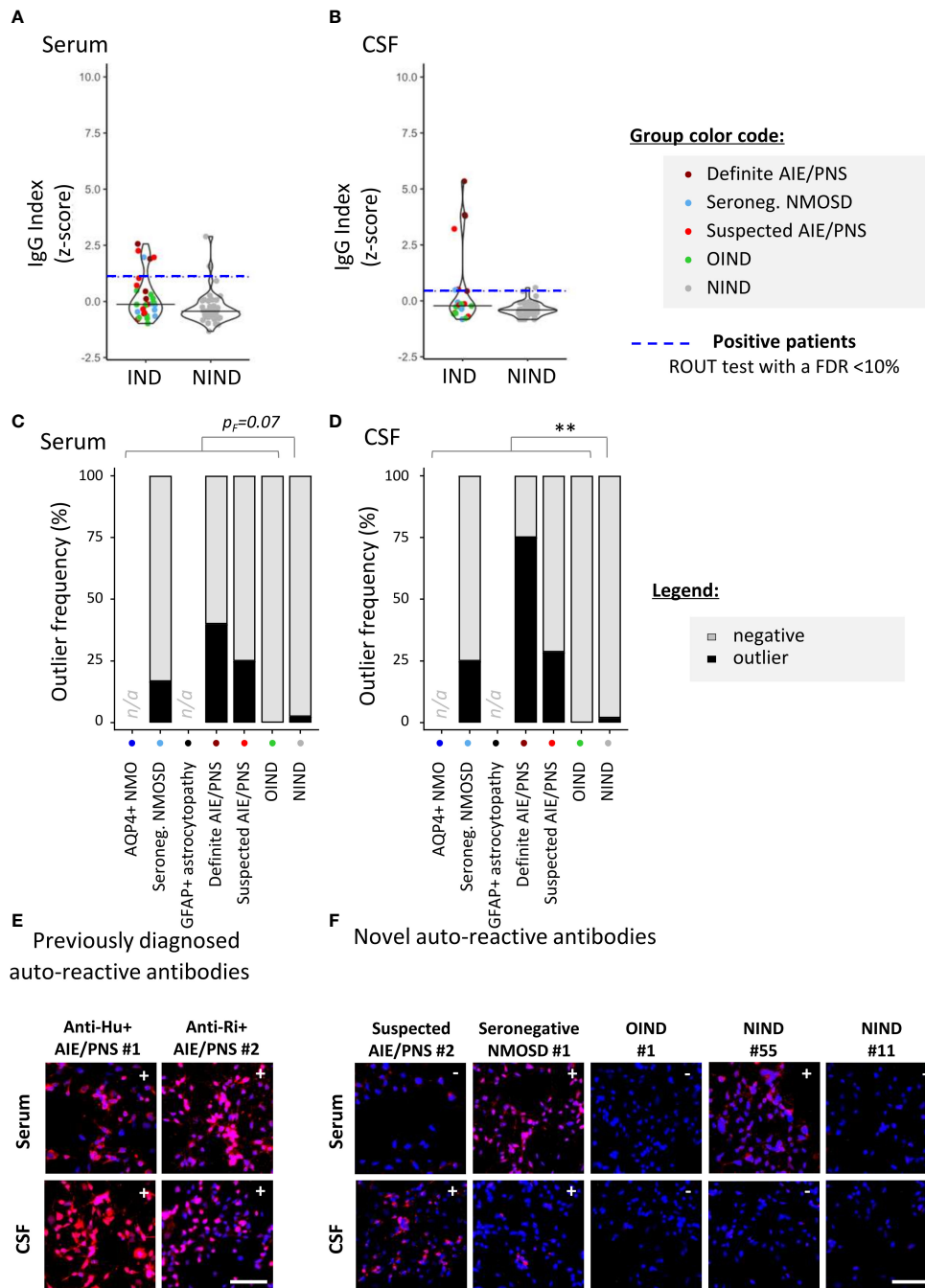
FIGURE 3

Detection of neuron-reactive IgG in sera and CSF of patients with a 96-well hiPSC-derived neuron cell-based assay (CBA). Human iPSC derived neurons were used to screen for CNS-reactive Abs associated with inflammatory and non-inflammatory neurological syndromes [inflammatory neurological disease, (IND) and non-IND (NIND), respectively]. Cells were exposed to selected serum and CSF (Figure 1). IgG-bound to neurons were detected in an intracellular 96-well CBA. **(A)** FI were assessed using a Synergy® microplate reader (left, serum; right, CSF). IgG indexes (z-score) are represented (see Methods for details). Each dot represents the mean of duplicates. The black plain lines represent the median of the group. Each clinical subgroups are represented in different colors. The blue dotted line represents the statistically determined limit above which outliers (defined as positive samples) were identified using a ROUT test with an FDR at<10% (see legend for color/group correspondence). **(B)** The frequency of outliers in each clinical subgroups are represented in black as bar graphs in the serum (left panel) or in the CSF (right panel). Differences in outlier frequencies between IND and NIND groups were tested using Fisher's exact test p_F: ns, $p > 0.05$; **$p < 0.01$. **(C, D)** Wells of the neuron-based CBA were observed by fluorescence microscopy. Representative microscopic observation is depicted for anti-Hu+ or anti-Ri+ PNS patients tested positive by validated diagnostic laboratories [**(C)**, expected intracellular IgG patterns] and for patients tested negative or not tested by validated diagnostic laboratories [**(D)**, intracellular IgG patterns]. The presence of IgG bound to neurons are detected in red, nuclei staining (DAPI) appears in blue. Symbols (+ or −) depicted in the upper right corner represent the results of CBA either positive outlier (+) or non-outliers (−) sample. White bars represent 50 μm. n/a, data not available.
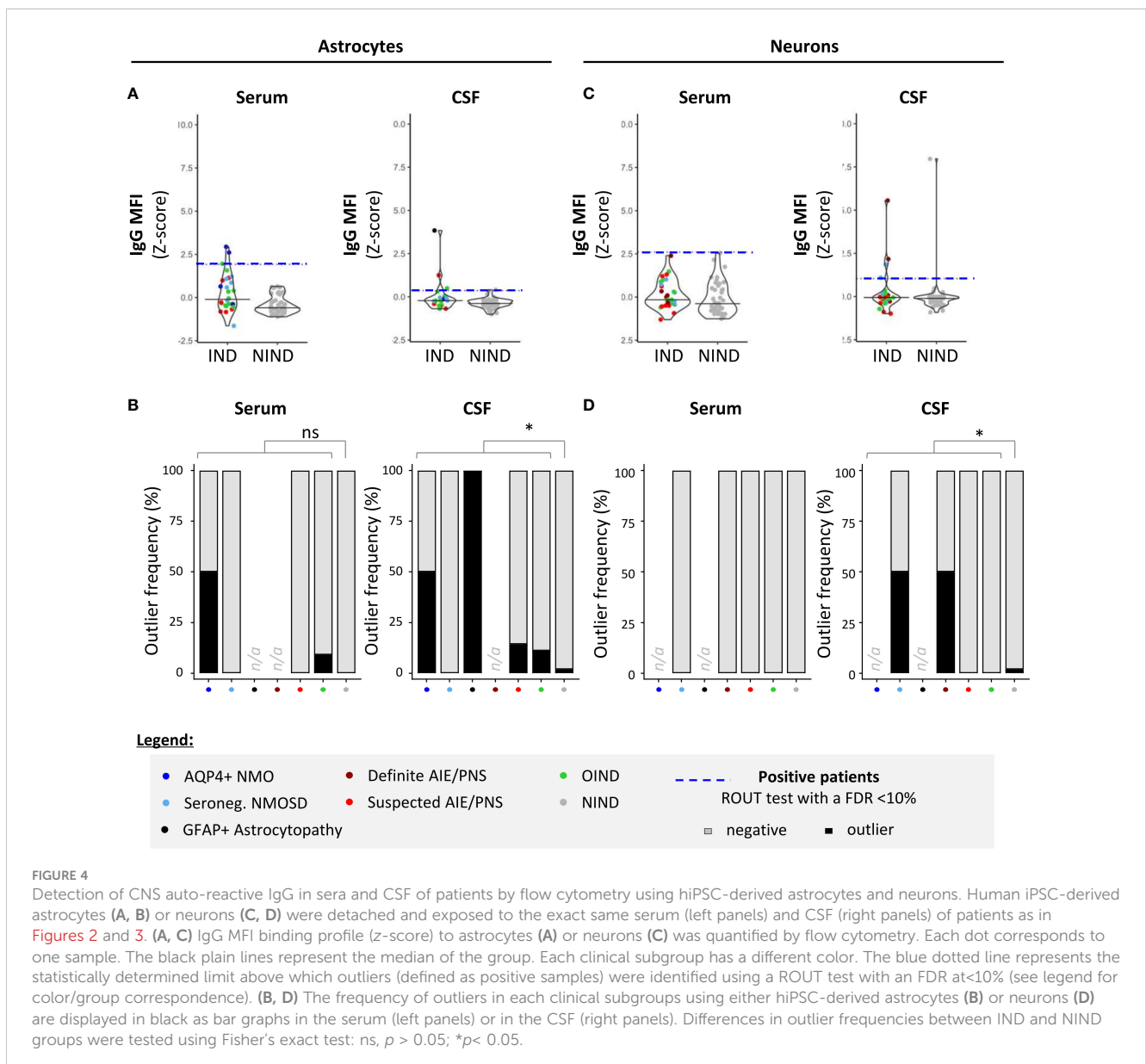
patients demonstrated any pattern specific of to-date reported CNS-reactive auto-Ab, supporting our human-based model as a complementary tool to detect new human CNS-reactive auto-Abs.
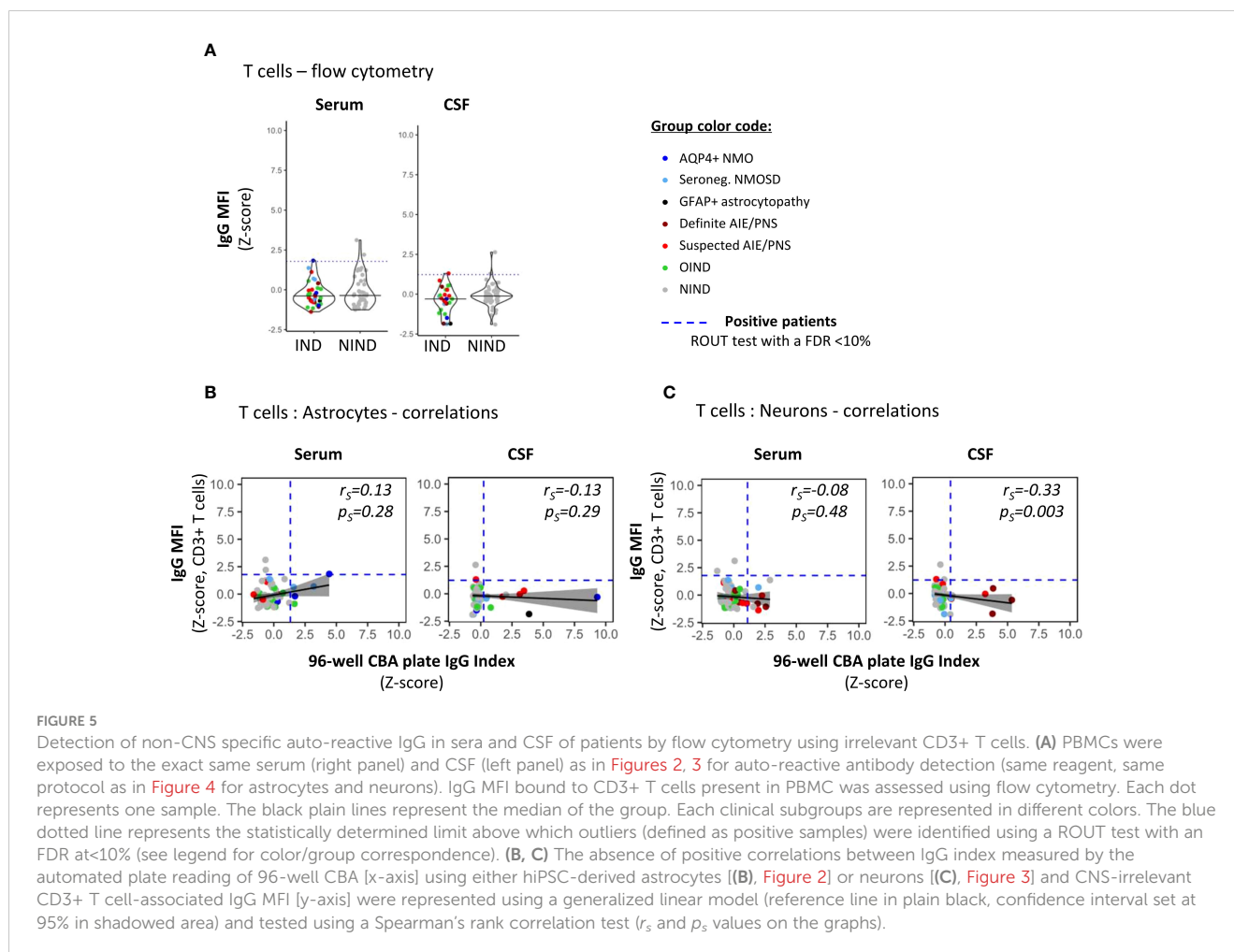
3.4 Comparison of 96-well CBA and flow cytometry measurements

To examine how our 96-well hiPSC-derived CNS CBA assessment (plate reader + fluorescence microscopy) would compare to flow cytometry measurements in the detection of CNS-reactive auto-Abs, we assessed the IgG-binding profile on detached hiPSC-derived astrocytes or neurons (Figure 4) or CD3+ T cells (the latter being used as control cells; Figure 5). All three cell types were exposed to the same selected serum and CSF samples and the IgG binding profile was assessed by quantifying IgG MFI.

Serum or CSF was defined as positive using a ROUT test with a FDR set at 10% on corresponding IgG MFI (z-score).

We found that there was a significant correlation between both astrocyte-based readouts, that is, 96-well hiPSC-derived CNS CBA and flow cytometry, but this correlation stood only when astrocytes were exposed to CSF and not to serum [plate reader: IgG index (z-score) vs. flow cytometry: IgG MFI (z-score)] (Spearman correlation statistics: serum, p_S= 0.15/r_S= 0.18; CSF, p_S= 0.03/r_S= 0.26). This positive correlation reinforces our hiPSC-derived astrocytes as a reliable source for the detection of astrocyte-specific auto-Abs. However, flow cytometry acquisition tended to be less sensitive than the 96-well hiPSC-derived astrocyte CBA. Comparing flow cytometry versus 96-well hiPSC-derived CNS CBA, we identified five of 34 versus nine of 36 IND and one of 57 versus three of 57 NIND, respectively (Figures 4A, B).

FIGURE 4
Detection of CNS auto-reactive IgG in sera and CSF of patients by flow cytometry using hiPSC-derived astrocytes and neurons. Human iPSC-derived astrocytes **(A, B)** or neurons **(C, D)** were detached and exposed to the exact same serum (left panels) and CSF (right panels) of patients as in Figures 2 and 3. **(A, C)** IgG MFI binding profile (z-score) to astrocytes **(A)** or neurons **(C)** was quantified by flow cytometry. Each dot corresponds to one sample. The black plain lines represent the median of the group. Each clinical subgroup has a different color. The blue dotted line represents the statistically determined limit above which outliers (defined as positive samples) were identified using a ROUT test with an FDR at<10% (see legend for color/group correspondence). **(B, D)** The frequency of outliers in each clinical subgroups using either hiPSC-derived astrocytes **(B)** or neurons **(D)** are displayed in black as bar graphs in the serum (left panels) or in the CSF (right panels). Differences in outlier frequencies between IND and NIND groups were tested using Fisher's exact test: ns, $p > 0.05$; *$p < 0.05$.

FIGURE 5

Detection of non-CNS specific auto-reactive IgG in sera and CSF of patients by flow cytometry using irrelevant CD3+ T cells. **(A)** PBMCs were exposed to the exact same serum (right panel) and CSF (left panel) as in Figures 2, 3 for auto-reactive antibody detection (same reagent, same protocol as in Figure 4 for astrocytes and neurons). IgG MFI bound to CD3+ T cells present in PBMC was assessed using flow cytometry. Each dot represents one sample. The black plain lines represent the median of the group. Each clinical subgroups are represented in different colors. The blue dotted line represents the statistically determined limit above which outliers (defined as positive samples) were identified using a ROUT test with an FDR at<10% (see legend for color/group correspondence). **(B, C)** The absence of positive correlations between IgG index measured by the automated plate reading of 96-well CBA [x-axis] using either hiPSC-derived astrocytes [**(B)**, Figure 2] or neurons [**(C)**, Figure 3] and CNS-irrelevant CD3+ T cell-associated IgG MFI [y-axis] were represented using a generalized linear model (reference line in plain black, confidence interval set at 95% in shadowed area) and tested using a Spearman's rank correlation test (r_s and p_s values on the graphs).

Regarding neurons, we observed no correlation between flow cytometry analyses MFI and 96-well CBA IgG index plate reader (Spearman correlation: serum p_S= 0.37/r_S= 0.11; CSF p_S= 0.08/r_S= 0.20). The less good yield of flow cytometry for this type of CNS cells is likely related to the detachment of hiPSC-derived neurons, a procedure that entails loss of neuronal structure, likely impairing Ag recognition by neuron-reactive auto-Abs. Indeed, comparing neuron-reactive IgG detected by flow cytometry versus 96-well hiPSC-derived CNS CBA, we identified four of 36 versus eight of 37 IND and four of 57 versus three of 57 NIND, respectively (Figures 4C, D). These findings align with previous reports indicating that flow cytometry is less sensitive as compared to live or fixed CBA, all of which are techniques commonly used for the diagnosis of Ab-related neurological conditions (35).

Finally, to confirm that serum and/or CSF IgG reactivity as defined by our 96-well hiPSC-derived CNS CBA was specifically directed toward CNS Ags, we assessed the IgG reactivity against primary irrelevant cells (CD3+ T cells) using a flow cytometry assay performed on the same serum/CSF samples (Figure 5). Notably, primary CD3+ T cells are naturally non-adherent cells thus flow cytometry acquisition represents an appropriate method to assess IgG binding profile (Figure 5A). The absence of any correlation between 96-well hiPSC-derived CNS CBA [IgG index (z-score)] and IgG reactivity to CD3+ T cells [IgG MFI (z-score)] strongly suggests that astrocyte- or neuron-IgG reactivities as identified by the 96-well hiPSC-derived CNS CBA are indeed limited to CNS Ags (Figures 5B, C).

In summary, our comprehensive 96-well hiPSC-derived CNS CBA appears to be a promising complementary approach to detect astrocyte- or neuron-specific Abs in the serum/CSF, of patients suspected to suffer from neurological conditions likely to be associated with an autoimmune/paraneoplastic etiology but who tested negative in reference diagnostic laboratories.

4 Discussion

Despite indisputable improvements in the diagnosis of immune-mediated neurological disorders facilitated by the detection of CNS-reactive Abs, there is still room for improvement. Indeed, physicians frequently encounter patients suspected of having neurological syndromes with an autoimmune etiology, yet no CNS-specific Abs are identified, even in reference laboratories (2, 3).

While hiPSC-derived neurons were previously used in peripheral autoimmune neurological or neuropsychiatric disorders (36, 37), we present a platform, namely a 96-well hiPSC-derived astrocyte- and neuron-CBA, enabling the rapid

detection of CNS-reactive Abs. This 96-well CBA yielded more robust results as compared to flow cytometry acquisition on detached hiPSC-derived astrocytes or neurons, consistent with other techniques used in validated laboratories (35). Using this 96-well CBA to detect CNS-reactive Abs, we identified nine patients with a reactivity profile restricted to astrocytes, eight to neurons, and two to both astrocytes and neurons. However, none exhibited detectable Ab binding to CD3+ T cells (used as non-CNS control cells), suggesting that the observed binding to neurons and/or astrocytes was specific to the neural Ags.

Importantly, we demonstrate that this unique 96-well CBA can partly replicate findings of established laboratories. More specifically, this assay caught an astrocyte-specific Ab response in one of one GFAP astrocytopathy and two of four AQP4+ NMOSD (two of two with positive AQP4-specific humoral immune response demonstrated in established laboratories at the same time as we performed our CBA assay). As per the two AQP4+ patients who tested negative in our 96-well hiPSC-derived astrocyte CBA, one was also negative and the other exhibited a low titer (1:32) in a reference lab. Furthermore, both were on immunomodulatory treatment (Mycophenolate Mofetil) for 7.1 years and 13.7 years at sampling date. It is known that AQP4+ positivity can be transitory in NMO, especially upon long-term immunosuppressive treatment. Indeed, over 3.7 years, one-third of the treated AQP4+ NMO patients seroreverts to AQP4 negative (38, 39).

The CBA assay also recapitulated a neuron-specific Ab response in three of four patients with established intracellular Ag-specific Abs (2 Hu+ AIE/PNS, 1 Ri+ AIE/PNS). In the patients who tested negative in the serum (no available CSF) with our CBA (AK5+ AIE), the antigenic target was detected with at a very low titer in validated diagnostic laboratories in both the serum and the CSF, a titer below the one we have set in our study. Indeed, when determining the level of dilution of IgG in serum and CSF, we deliberately selected a high dilution level to minimize false positive results and thus maximize the likelihood of detecting true positive ones. There were two additional patients with established AIE/PNS: one NMDAR and one PCA-Tr, whose Ags are expressed on the surface, respectively on the synapse, for whom we detected no reactive Abs either in the serum or the CSF. Indeed, our CBA entails permeabilization of the cells, which could potentially interfere with surface/synaptic Ag detection. These data suggest that our CBA assay is more able to detect intra-cellular than surface Ags and would thus make it particularly suitable for the search of CNS-specific intracellular Ag, such as in paraneoplastic conditions. Additionally, our protocol to obtain hiPSC-derived neurons does not generate Purkinje cells, possibly preventing from the detection of PCA-Tr+ auto-Abs. Detection of surface or synaptic Ags may rely on live CBA, requiring further refinements for future investigations.

Such as mentioned above, in the validation cohort, we were able to replicate findings of established laboratories in confirmed cases of NMO AQP4+ (two of four) and definite AIE/PNS (four of seven, in particular when the Ag was intracellular), which helped to validate our 96-well hiPSC derived CBA. Nevertheless, our assay does not intend to replace existing first-line diagnostic tests, which explains why sensitivity assessments were not considered. Instead, it is important to keep in mind that our assay is positioned as a second-step test in clinically-suspected cases for whom

conventional tests are negative. Most interestingly, beyond seropositive AQP4+ NMO and definite AIE/PNS, we identified astrocyte- and neuron-reactive Abs in seronegative NMOSD (two of six), suspected AIE/PNS (six of 12), OIND (one of 13), and NIND (four of 57). For these patients, CNS-specific Abs were not reported at the time of blood sampling yet, including nine IND and four NIND patients. Remarkably, two of four NIND patients (NIND #23 suffering from inclusion body myositis; NIND#37 suffering from non-ischemic cerebral enhancing [NICE]) exhibited astrocyte- or neuron- reactive Abs, respectively. We cannot rule out that these two patients may have suffered from autoimmune conditions. Indeed, inclusion body myositis has sometimes been associated with intracellular auto-Abs targeting the cytosolic 5'-nucleotidase 1A (cN1A; NT5C1A) (40), a protein expressed in the periphery by muscle cells and cardiomyocyte and in the CNS by some astrocytes and neurons. NICE condition, a rare complication after endovascular therapy, was associated in this patient with post-subarachnoid hemorrhage. Interestingly, NICE may be associated with inflammatory non-specific lymphocyte infiltration in the brain (41) and CSF (42) along with reactive astrocyte (41). Nevertheless, we decided to remain conservative and classified the NICE patient into the NIND category as there was no increased leukocyte count in the CSF. Furthermore, one patient (NIND #3), who suffered from amyotrophic lateral sclerosis (ALS) showed a distinct astrocyte-binding reactivity as compared to the other astrocyte-reactive NIND patient. This observation is supported by recent observations of neural auto-Abs in ALS (43, 44). However, in the two NIND patients (NIND#23 suffering from NICE; NIND#55 suffering from stroke) exhibiting a reactivity against neurons, the latter was restricted to the serum, contrasting to what was observed in most of IND patients for whom both serum and CSF were detected positive when paired samples were tested. In line with this observation, using the CBA, the intensity of the CNS-reactive IgG response was more intense in IND than in NIND patients, either when it was directed against astrocytes (in serum the astrocyte-reactivity was present only in IND; CSF IND 2.47-fold higher than NIND) or against neurons (serum IND 1.25-fold higher than NIND; CSF IND 4.69-fold higher than NIND). Additionally, we found that the CSF is a better compartment than the serum to screen for CNS-reactive Ab. These findings support recent reports emphasizing the importance of CSF testing for accurate diagnostic interpretation, particularly neuronal Ab reactivity (45–47). Noteworthy, the patients for whom we newly identified astrocyte- and/or neuron-reactivity with our 96-well hiPSC-derived CNS CBA, all had a negative result using mouse tissue as an Ab detection method in a reference lab. These findings thus support our human-based model as a complementary tool for the identification of not yet reported CNS-reactive Abs in patients with a strong suspicion of CNS autoimmune disease. Worth noting, the presence of neural auto-Abs in the serum but not in the CSF of healthy controls has been reported with variable low frequencies (0.23%–2%) (48, 49). Thus, future studies using our hiPSC-derived CBA should include data from larger cohorts, including, if possible, CSF of healthy donors, to test the specificity of our tool to detect novel neural-specific auto-Abs.

Interestingly, we and others have demonstrated that direct neuronal differentiation from neural progenitors (NPC) using

NGN2-inducible protocol allows for the rapid and highly reproducible differentiation of mixed neuronal population (27, 29, 50, 51). While for some experimental purposes, this heterogeneity may be concerning (for instance for genetic studies where a very precise type of neuron needs to be studied) (50), we consider that this feature may be an asset for our approach. Indeed, the highest antigenic diversity increases the chance to detect an Ab response.

One could argue that this CBA is currently restricted to astrocytes and neurons. Including other CNS cell types such as oligodendrocytes (52), microglia (53), endothelial (54) or even ependymal cells (55) to broaden antigenic diversity would certainly be an asset. However, astrocytes and neurons currently cover the vast majority of the CNS Ags to be associated with neurological disorders (56). MOG is the only Ag not expressed by astrocytes and/or neurons, but by oligodendrocytes (10). Recently, authors have relied on new elegant peptide-based techniques such as phage-based techniques to detect CNS-reactive auto-Abs and their cognate Ags (57–61). Nevertheless, even though these proteome-wide auto-Ab discovery platforms are unbiased, these techniques are not ideal for detecting proteins in their 3D conformation as they do not consider post-translational protein modifications (62). However, these parameters are crucial for Ab-Ag recognition (63–65). We think that our unique human hiPSC-based platform may serve as a complementary testing tool in patients with a clinical presentation suggestive for CNS-reactive Ab-mediated disease but in whom no anti-CNS cell Abs were detected in validated routine laboratory testing.

Beyond this testing, our platform could offer the possibility to identify previously unreported CNS Ags targeted by CNS-reactive Abs especially when considering intracellular Ag(s). Ultimately, our rapid 96-well hiPSC-derived CNS platform offers a promising avenue for further investigations ultimately translating into a potential support for a better diagnosis and therapeutical management of auto-Ab–related neurological conditions.

Data availability statement

The raw data supporting the conclusions of this article will be made available by the authors, without undue reservation.

Ethics statement

The studies involving humans were approved by Commission cantonale d'éthique de la recherche sur l'être humain (CER-VD). The studies were conducted in accordance with the local legislation and institutional requirements. The participants provided their written informed consent to participate in this study. Ethical approval was not required for the study involving animals in accordance with the local legislation and institutional requirements because this study used commercially available slide with cryosectioned composite of murine tissues (Scimedx Corporation, Denville, USA).

Conflict of interest

RBV received travel grants from Roche and received speaker honoraria from Novartis. None were related to this work. AH has served as an expert in advisory boards from Novocure and Bayer and received speaker honoraria from Novocure, all paid to the institution and not related to this work. AZ has patents submitted for Tensacin-R IgG, PDE10A-IgG, and DACH1-IgG as biomarkers of neurological autoimmunity, receives research funding from Roche/Genetech non-relevant to this work, and has consulted for Alexion Pharmaceutical without personal compensation. MT has

served as an expert in advisory boards for Biogen, Genzyme-Sanofi, Merck, Novartis, and Roche; received travel grants from Biogen, Genzyme-Sanofi, Merck, Novartis, and Roche; and received speaker honoraria from Biogen, Novartis, and Merck. None were related to this work. CP has served as an expert in advisory boards and received travel grants from Biogen, Genzyme-Sanofi, Merck, Novartis, and Roche. None were related to this work. RDP has served on scientific advisory boards for Biogen, BMS, Merck, Novartis, Roche, and Sanofi-Genzyme and has received funding for travel or speaker honoraria from Biogen, Merck, Roche, and Sanofi-Genzyme.

The remaining authors declare that the research was conducted in the absence of any commercial or financial relationships that could be construed as a potential conflict of interest.

Publisher's note

All claims expressed in this article are solely those of the authors and do not necessarily represent those of their affiliated organizations, or those of the publisher, the editors and the reviewers. Any product that may be evaluated in this article, or claim that may be made by its manufacturer, is not guaranteed or endorsed by the publisher.

Supplementary material

The Supplementary Material for this article can be found online at: https://www.frontiersin.org/articles/10.3389/fimmu.2024.1419712/full#supplementary-material.

References

1. Mader S, Brimberg L, Diamond B. The role of brain-reactive autoantibodies in brain pathology and cognitive impairment. *Front Immunol*. (2017) 8:1101. doi: 10.3389/fimmu.2017.01101

2. Prüss H. Autoantibodies in neurological disease. *Nat Rev Immunol*. (2021) 21:798–813. doi: 10.1038/s41577-021-00543-w

3. Graus F, Titulaer MJ, Balu R, Benseler S, Bien CG, Cellucci T, et al. A clinical approach to diagnosis of autoimmune encephalitis. *Lancet Neurology*. (2016) 15:391–404. doi: 10.1016/S1474-4422(15)00401-9

4. Zekeridou A, Rossetti AO, Hottinger AF, Du Pasquier RA. [Anti-neuronal antibodies: a rapidly developing field]. *Rev Med Suisse*. (2013) 9:909–14.

5. Dubey D, Pittock SJ, Kelly CR, McKeon A, Lopez-Chiriboga AS, Lennon VA, et al. Autoimmune encephalitis epidemiology and a comparison to infectious encephalitis. *Ann Neurology*. (2018) 83:166–77. doi: 10.1002/ana.25131

6. Graus F, Escudero D, Oleaga L, Bruna J, Villarejo-Galende A, Ballabriga J, et al. Syndrome and outcome of antibody-negative limbic encephalitis. *Eur J Neurology*. (2018) 25:1011–6. doi: 10.1111/ene.13661

7. Gastaldi M, Mariotto S, Giannoccaro MP, Iorio R, Zoccarato M, Nosadini M, et al. Subgroup comparison according to clinical phenotype and serostatus in autoimmune encephalitis: a multicenter retrospective study. *Eur J Neurol*. (2020) 27:633–43. doi: 10.1111/ene.14139

8. Emma O, Cristina V-S, Jeffrey B, Divyanshu D, Eoin PF, Lopez-Chiriboga AS, et al. Autoimmune encephalitis criteria in clinical practice. *Neurology: Clin Practice*. (2023) 13:e200151. doi: 10.1212/CPJ.0000000000200151

9. Hyun JW, Jeong IH, Joung A, Kim SH, Kim HJ. Evaluation of the 2015 diagnostic criteria for neuromyelitis optica spectrum disorder. *Neurology*. (2016) 86:1772–9. doi: 10.1212/WNL.0000000000002655

10. Hamid SHM, Whittam D, Mutch K, Linaker S, Solomon T, Das K, et al. What proportion of AQP4-IgG-negative NMO spectrum disorder patients are MOG-IgG positive? A cross sectional study of 132 patients. *J Neurology*. (2017) 264:2088–94. doi: 10.1007/s00415-017-8596-7

11. Lee W-J, Lee H-S, Kim D-Y, Lee H-S, Moon J, Park K-I, et al. Seronegative autoimmune encephalitis: clinical characteristics and factors associated with outcomes. *Brain*. (2022) 145:3509–21. doi: 10.1093/brain/awac166

12. Wingerchuk DM, Banwell B, Bennett JL, Cabre P, Carroll W, Chitnis T, et al. International consensus diagnostic criteria for neuromyelitis optica spectrum disorders. *Neurology*. (2015) 85:177–89. doi: 10.1212/WNL.0000000000001729

13. Lenti MV, Rossi CM, Melazzini F, Gastaldi M, Bugatti S, Rotondi M, et al. Seronegative autoimmune diseases: A challenging diagnosis. *Autoimmun Rev*. (2022) 21:103143. doi: 10.1016/j.autrev.2022.103143

14. Güre AO, Stockert E, Scanlan MJ, Keresztes RS, Jäger D, Altorki NK, et al. Serological identification of embryonic neural proteins as highly immunogenic tumor antigens in small cell lung cancer. *Proc Natl Acad Sci*. (2000) 97:4198–203. doi: 10.1073/pnas.97.8.4198

15. Vincent A. ANTIBODIES AND RECEPTORS: from neuromuscular junction to central nervous system. *Neuroscience*. (2020) 439:48–61. doi: 10.1016/j.neuroscience.2020.03.009

16. Scharf M, Miske R, Kade S, Hahn S, Denno Y, Begemann N, et al. A spectrum of neural autoantigens, newly identified by histo-immunoprecipitation, mass spectrometry, and recombinant cell-based indirect immunofluorescence. *Front Immunol*. (2018) 9:1447–. doi: 10.3389/fimmu.2018.01447

17. Banjara M, Ghosh C, Dadas A, Mazzone P, Janigro D. Detection of brain-directed autoantibodies in the serum of non-small cell lung cancer patients. *PloS One*. (2017) 12:e0181409. doi: 10.1371/journal.pone.0181409

18. Iffland PH, Carvalho-Tavares J, Trigunaite A, Man S, Rasmussen P, Alexopoulos A, et al. Intracellular and circulating neuronal antinuclear antibodies in human epilepsy. *Neurobiol Disease*. (2013) 59:206–19. doi: 10.1016/j.nbd.2013.07.006

19. Farahany NA, Greely HT, Hyman S, Koch C, Grady C, Paşca SP, et al. The ethics of experimenting with human brain tissue. *Nature*. (2018) 556:429–32. doi: 10.1038/d41586-018-04813-x

20. Harschnitz O. Human stem cell–derived models: lessons for autoimmune diseases of the nervous system. *Neuroscientist*. (2019) 25:199–207. doi: 10.1177/1073858418777999

21. Graus F, Vogrig A, Muñiz-Castrillo S, Antoine J-CG, Desestret V, Dubey D, et al. Updated diagnostic criteria for paraneoplastic neurologic syndromes. *Neurol Neuroimmunology Neuroinflammation*. (2021) 8:e1014. doi: 10.1212/NXI.0000000000001014

22. Perriot S, Mathias A, Perriard G, Canales M, Jonkmans N, Merienne N, et al. Human induced pluripotent stem cell-derived astrocytes are differentially activated by multiple sclerosis-associated cytokines. *Stem Cell Rep*. (2018) 11:1199–210. doi: 10.1016/j.stemcr.2018.09.015

23. Perriot S, Canales M, Mathias A, Du Pasquier R. Differentiation of functional astrocytes from human-induced pluripotent stem cells in chemically defined media. *STAR Protoc*. (2021) 2:100902. doi: 10.1016/j.xpro.2021.100902

24. Perriot S, Canales M, Mathias A, Du Pasquier R. Generation of transgene-free human induced pluripotent stem cells from erythroblasts in feeder-free conditions. *STAR Protoc*. (2022) 3:101620. doi: 10.1016/j.xpro.2022.101620

25. Ho SM, Hartley BJ, Tcw J, Beaumont M, Stafford K, Slesinger PA, et al. Rapid Ngn2-induction of excitatory neurons from hiPSC-derived neural progenitor cells. *Methods*. (2016) 101:113–24. doi: 10.1016/j.ymeth.2015.11.019

26. Oberholster L, Mathias A, Perriot S, Blaser E, Canales M, Jones S, et al. Comprehensive proteomic analysis of JC polyomavirus-infected human astrocytes and their extracellular vesicles. *Microbiol Spectr*. (2023) 11(6):e0275123. doi: 10.1128/spectrum.02751-23

27. Bibert S, Quinodoz M, Perriot S, Krebs FS, Jan M, Malta RC, et al. Herpes simplex encephalitis due to a mutation in an E3 ubiquitin ligase. *Nat Commun*. (2024) 15:3969. doi: 10.1038/s41467-024-48287-0

28. Callegari I, Oechtering J, Schneider M, Perriot S, Mathias A, Voortman MM, et al. Cell-binding IgM in CSF is distinctive of multiple sclerosis and targets the iron transporter SCARA5. *Brain*. (2023) 147(3):839–48. doi: 10.1101/2023.09.29.560121

29. Perriot S, Samuel J, Raphael G, Amandine M, Helen L, Sara B, et al. KIR3DL1 and Tox identify clonally expanded encephalitogenic neuron-specific CD8+ T cells in autoimmune encephalitis. *bioRxiv*. (2024). doi: 10.1101/2024.03.25.586688

30. Stirling DR, Swain-Bowden MJ, Lucas AM, Carpenter AE, Cimini BA, Goodman A. CellProfiler 4: improvements in speed, utility and usability. *BMC Bioinf*. (2021) 22:433. doi: 10.1186/s12859-021-04344-9

31. Dao D, Fraser AN, Hung J, Ljosa V, Singh S, Carpenter AE. CellProfiler Analyst: interactive data exploration, analysis and classification of large biological image sets. *Bioinformatics*. (2016) 32:3210–2. doi: 10.1093/bioinformatics/btw390

32. Perriard G, Mathias A, Enz L, Canales M, Schluep M, Gentner M, et al. Interleukin-22 is increased in multiple sclerosis patients and targets astrocytes. *J Neuroinflammation*. (2015) 12:119. doi: 10.1186/s12974-015-0335-3

33. Jilek S, Schluep M, Meylan P, Vingerhoets F, Guignard L, Monney A, et al. Strong EBV-specific CD8+ T-cell response in patients with early multiple sclerosis. *Brain*. (2008) 131:1712–21. doi: 10.1093/brain/awn108

34. Zekeridou A, Kryzer T, Guo Y, Hassan A, Lennon V, Lucchinetti CF, et al. Phosphodiesterase 10A IgG: A novel biomarker of paraneoplastic neurologic autoimmunity. *Neurology*. (2019) 93:e815–e22. doi: 10.1212/WNL.0000000000007971

35. Ramberger M, Peschl P, Schanda K, Irschick R, Höftberger R, Deisenhammer F, et al. Comparison of diagnostic accuracy of microscopy and flow cytometry in evaluating N-methyl-D-aspartate receptor antibodies in serum using a live cell-based assay. *PloS One*. (2015) 10:e0122037. doi: 10.1371/journal.pone.0122037

36. Harschnitz O, van den Berg LH, Johansen LE, Jansen MD, Kling S, Vieira de Sá R, et al. Autoantibody pathogenicity in a multifocal motor neuropathy induced pluripotent stem cell–derived model. *Ann Neurology*. (2016) 80:71–88. doi: 10.1002/ana.24680

37. Pan H, Oliveira B, Saher G, Dere E, Tapken D, Mitjans M, et al. Uncoupling the widespread occurrence of anti-NMDAR1 autoantibodies from neuropsychiatric disease in a novel autoimmune model. *Mol Psychiatry*. (2019) 24:1489–501. doi: 10.1038/s41380-017-0011-3

38. Yin H-X, Wang Y-J, Liu M-G, Zhang D-D, Ren H-T, Mao Z-F, et al. Aquaporin-4 antibody dynamics and relapse risk in seropositive neuromyelitis optica spectrum disorder treated with immunosuppressants. *Ann Neurology*. (2023) 93:1069–81. doi: 10.1002/ana.26623

39. Majed M, Valencia Sanchez C, Bennett JL, Fryer J, Mulligan MD, Redenbaugh V, et al. Alterations in aquaporin-4-igG serostatus in 986 patients: A laboratory-based longitudinal analysis. *Ann Neurology*. (2023) 94:727–35. doi: 10.1002/ana.26722

40. Larman HB, Salajegheh M, Nazareno R, Lam T, Sauld J, Steen H, et al. Cytosolic 5'-nucleotidase 1A autoimmunity in sporadic inclusion body myositis. *Ann Neurol*. (2013) 73:408–18. doi: 10.1002/ana.23840

41. Shotar E, Law-Ye B, Baronnet-Chauvet F, Zeidan S, Psimaras D, Bielle F, et al. Non-ischemic cerebral enhancing lesions secondary to endovascular aneurysm therapy: nickel allergy or foreign body reaction? Case series and review of the literature. *Neuroradiology*. (2016) 58:877–85. doi: 10.1007/s00234-016-1699-5

42. Shapiro M, Ollenschleger MD, Baccin C, Becske T, Spiegel GR, Wang Y, et al. Foreign body emboli following cerebrovascular interventions: clinical, radiographic, and histopathologic features. *Am J Neuroradiology*. (2015) 36:2121–6. doi: 10.3174/ajnr.A4415

43. Stevens-Jones O, Malmeström C, Constantinescu C, Dalla K, Nellgård B, Zelano J, et al. Presence of neural surface and onconeural autoantibodies in cerebrospinal fluid and serum in neurological diseases presents a potential risk for misdiagnosis. *Eur J Neurology*. (2023) 30:2602–10. doi: 10.1111/ene.15926

44. Häggmark A, Mikus M, Mohsenchian A, Hong MG, Forsström B, Gajewska B, et al. Plasma profiling reveals three proteins associated to amyotrophic lateral sclerosis. *Ann Clin Trans neurology*. (2014) 1:544–53. doi: 10.1002/acn3.83

45. Gresa-Arribas N, Titulaer MJ, Torrents A, Aguilar E, McCracken L, Leypoldt F, et al. Antibody titres at diagnosis and during follow-up of anti-NMDA receptor encephalitis: a retrospective study. *Lancet Neurol*. (2014) 13:167–77. doi: 10.1016/S1474-4422(13)70282-5

46. Budhram A, Dubey D, Sechi E, Flanagan EP, Yang L, Bhayana V, et al. Neural antibody testing in patients with suspected autoimmune encephalitis. *Clin Chem*. (2020) 66:1496–509. doi: 10.1093/clinchem/hvaa254

47. Balint B, Bhatia KP, Dalmau J. Antibody of unknown significance" (AUS): the issue of interpreting antibody test results. *Mov Disord*. (2021) 36:1543–7. doi: 10.1002/mds.28597

48. Lang K, Prüss H. Frequencies of neuronal autoantibodies in healthy controls: Estimation of disease specificity. *Neurology(R) neuroimmunology neuroinflammation*. (2017) 4:e386. doi: 10.1212/NXI.0000000000000386

49. Dahm L, Ott C, Steiner J, Stepniak B, Teegen B, Saschenbrecker S, et al. Seroprevalence of autoantibodies against brain antigens in health and disease. *Ann Neurology*. (2014) 76:82–94. doi: 10.1002/ana.24189

50. Hulme AJ, Maksour S, St-Clair Glover M, Miellet S, Dottori M. Making neurons, made easy: The use of Neurogenin-2 in neuronal differentiation. *Stem Cell Rep*. (2022) 17:14–34. doi: 10.1016/j.stemcr.2021.11.015

51. Lin H-C, He Z, Ebert S, Schörnig M, Santel M, Nikolova MT, et al. NGN2 induces diverse neuron types from human pluripotency. *Stem Cell Rep*. (2021) 16:2118–27. doi: 10.1016/j.stemcr.2021.07.006

52. García-León JA, García-Díaz B, Eggermont K, Cáceres-Palomo L, Neyrinck K, Madeiro da Costa R, et al. Generation of oligodendrocytes and establishment of an all-human myelinating platform from human pluripotent stem cells. *Nat Protoc*. (2020) 15:3716–44. doi: 10.1038/s41596-020-0395-4

53. Sonn I, Honda-Ozaki F, Yoshimatsu S, Morimoto S, Watanabe H, Okano H. Single transcription factor efficiently leads human induced pluripotent stem cells to functional microglia. *Inflammation Regeneration*. (2022) 42:20. doi: 10.1186/s41232-022-00201-1

54. Nishihara H, Gastfriend BD, Soldati S, Perriot S, Mathias A, Sano Y, et al. Advancing human induced pluripotent stem cell-derived blood-brain barrier models for studying immune cell interactions. *FASEB J*. (2020) 34:16693–715. doi: 10.1096/fj.202001507RR

55. Redmond SA, Figueres-Oñate M, Obernier K, Nascimento MA, Parraguez JI, López-Mascaraque L, et al. Development of ependymal and postnatal neural stem cells and their origin from a common embryonic progenitor. *Cell Rep*. (2019) 27:429–41.e3. doi: 10.1016/j.celrep.2019.01.088

56. Sechi E, Flanagan EP. Antibody-mediated autoimmune diseases of the CNS: challenges and approaches to diagnosis and management. *Front neurology*. (2021) 12:673339. doi: 10.3389/fneur.2021.673339

57. Mandel-Brehm C, Dubey D, Kryzer TJ, O'Donovan BD, Tran B, Vazquez SE, et al. Kelch-like protein 11 antibodies in seminoma-associated paraneoplastic encephalitis. *New Engl J Med*. (2019) 381:47–54. doi: 10.1056/NEJMoa1816721

58. Bartley CM, Ngo TT, Do LD, Zekeridou A, Dandekar R, Muñiz-Castrillo S, et al. Detection of high-risk paraneoplastic antibodies against TRIM9 and TRIM67 proteins. *Ann Neurol*. (2023) 94:1086–101. doi: 10.1002/ana.26776

59. McKeon A, Lesnick C, Vorasoot N, Buckley MW, Dasari S, Flanagan EP, et al. Utility of protein microarrays for detection of classified and novel antibodies in autoimmune neurologic disease. *Neurology(R) neuroimmunology Neuroinflamm*. (2023) 10. doi: 10.1212/NXI.0000000000200145

60. Rezk M, Pittock SJ, Kapadia RK, Knight AM, Guo Y, Gupta P, et al. Identification of SKOR2 IgG as a novel biomarker of paraneoplastic neurologic syndrome. *Front Immunol*. (2023) 14:1243946. doi: 10.3389/fimmu.2023.1243946

61. Larman HB, Zhao Z, Laserson U, Li MZ, Ciccia A, Gakidis MA, et al. Autoantigen discovery with a synthetic human peptidome. *Nat Biotechnol*. (2011) 29:535–41. doi: 10.1038/nbt.1856

62. Wang EY, Dai Y, Rosen CE, Schmitt MM, Dong MX, Ferré EMN, et al. High-throughput identification of autoantibodies that target the human exoproteome. *Cell Rep Methods*. (2022) 2:100172. doi: 10.1016/j.crmeth.2022.100172

63. Lanz TV, Brewer RC, Ho PP, Moon J-S, Jude KM, Fernandez D, et al. Clonally expanded B cells in multiple sclerosis bind EBV EBNA1 and GlialCAM. *Nature*. (2022) 603:321–7. doi: 10.1038/s41586-022-04432-7

64. Sinmaz N, Nguyen T, Tea F, Dale RC, Brilot F. Mapping autoantigen epitopes: molecular insights into autoantibody-associated disorders of the nervous system. *J Neuroinflammation*. (2016) 13:219. doi: 10.1186/s12974-016-0678-4

65. Ricken G, Schwaiger C, De Simoni D, Pichler V, Lang J, Glatter S, et al. Detection methods for autoantibodies in suspected autoimmune encephalitis. *Front neurology*. (2018) 9:841. doi: 10.3389/fneur.2018.00841